New principle for optical tomography and profilometry based on spatial coherence synthesis with a spatially modulated extended light source

Wei Wang[a,b**], Hirokazu Kozaki[b*], Joseph Rosen[c***], and Mitsuo Takeda[b*]

[a]Department of Physics, University of Science and Technology of China
[b]Department of Information and Communication Engineering,
The University of Electro-Communications
[c]Department of Electrical and Computer Engineering, Ben-Gurion University of the Negev

ABSTRACT

Giving a new physical interpretation to the principle of longitudinal coherence control, we propose an improved method for synthesizing a desired spatial coherence function along the longitudinal axis of light propagation. By controlling the irradiance of an extended quasi-monochromatic spatially incoherent source with a spatial light modulator, we generated a special optical field that exhibits high coherence selectively for the particular pair of points at the specified locations along the axis of beam propagation. This function of longitudinal coherence control provides new possibilities in optical tomography and profilometry. Quantitative experimental proof of the principle is presented.

Keywords: Coherence Tomography, Interferometry, Profilometry, Spatial Coherence, Interferometer, Coherence Theory

1. INTRODUCTION

Optical coherence tomography [1,2] and low-coherence profilometry [3,4] have been studied extensively. They use the physical property of broadband light that high contrast fringes can be observed only when the beams from the sample and the reference mirror have the same optical path lengths. In other words, they are based on the common basic principle in which the characteristic of longitudinal coherence plays a crucial role. Usually the term longitudinal coherence is identified with temporal coherence [5], where coherence between two points along the propagation axis is determined by the temporal spectrum of the radiating source. However, if one notes the analogies between temporal and spatial parameters that are found in many optical phenomena [6], one may think of yet another scheme for controlling longitudinal coherence by changing the spatial (rather than temporal) structure of the radiating source. McCutchen[7],

Rosen and Yariv [8,9] have shown that the longitudinal coherence between two points along the propagation axis can be determined purely by the spatial structure of a quasi-monochromatic incoherent planar source. In analogy to that the Wiener-Khintchine theorem relates the temporal coherence to the source spectrum, the generalized Van Cittert-Zernike theorem [8,9] relates the longitudinal spatial coherence to the spatial structure of the extended source. More recently, Rosen and Takeda [10] proposed a new scheme of surface profilometry based on the longitudinal spatial coherence. Whereas the conventional coherence tomography and the low-coherence profilometry use a spectrally broad (i.e., temporally incoherent) and spatially confined (i.e., spatially coherent) point source (e.g., a super luminescent diode), our technique uses a spectrally narrow (i.e., quasi-monochromatic and temporally coherent) and spatially extended (i.e., spatially incoherent) source. The use of the narrow-band source can be an advantage when the object and/or the medium through which the light propagates have strong dispersion and/or inhomogeneous spectral absorption. The system requires no optical elements for dispersion correction (such as a dispersion compensation glass plate in a white-light Michelson interferometer). If a highly absorbing object or medium has a low-absorbing spectral window, the use of the quasi-monochromatic source permits one to tune the spectrum to the low-absorbing spectral window. The conventional coherence tomography and the low-coherence profilometry require mechanical movement of the reference mirror for the change of the optical path difference because their longitudinal (temporal) coherence function is invariable as it is determined by the spectrum of the light source. The proposed technique is free from the mechanism for changing the optical path difference because the longitudinal (spatial) coherence function is varied with a spatial light modulator in such a manner that the high contrast fringes are observed at the desired optical path difference. In the sense of space-time analogy [6], our scheme for synthesizing spatial coherence is conceptually analogous to the synthesis of temporal coherence proposed by Hotate and Okugawa [11], though the specific techniques used are completely different.

2. PRINCIPLE

2.1 Description by Fourier optics

The schematic diagram of the proposed system is illustrated in Fig.1. A Michelson interferometer is illuminated by an extended quasi-monochromatic spatially incoherent light source S located at the front focal plane of lens L1.

Light emitted from a point A(x_s, y_s) of the source is collimated by the lens L1, and is split into two beams by beam splitter BS. One beam is reflected from mirror M1 that serves as an object, and the other from mirror M2 that serves as a reference. The mirrors M1 and M2 are located at distance $z = L$ and $z = L + \Delta z$, respectively, from the rear focal plane of the collimating lens L1. The interference fringes generated on the CCD image sensor are the result of combining the images of the two optical field distributions; one is the optical field distribution at the object mirror M1 and the other is the optical field distribution created at the corresponding location in the reference arm by the reference mirror M2. The both images are obtained by the imaging lens L2, and the CCD image sensor records the intensity of these fringes.

The point source, with complex amplitude $u_s(x_s, y_s)$ at A, creates behind the lens L1 a field distribution
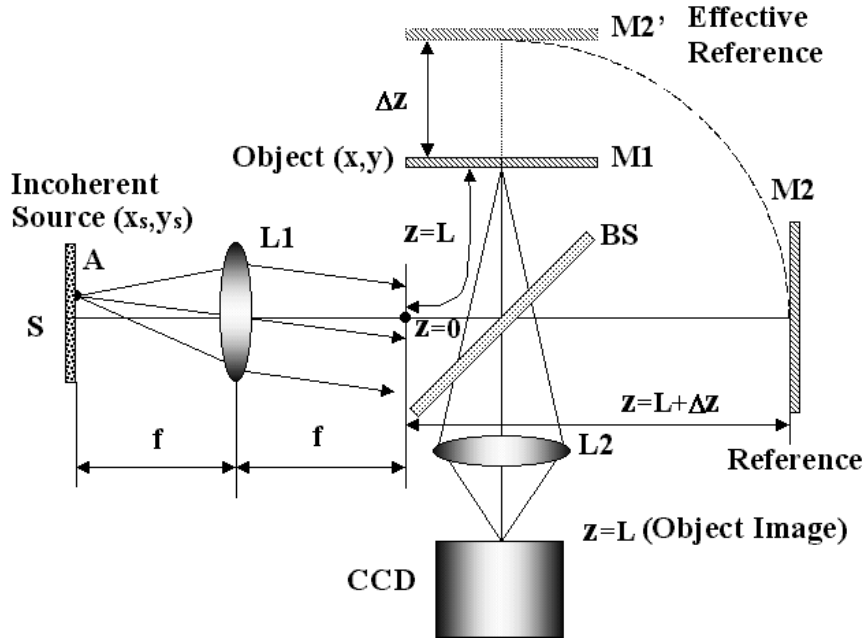
Fig. 1   Optical system for measuring longitudinal complex degree of coherence.

$$u(x, y, z) = \frac{u_s(x_s, y_s)}{j\lambda f} \exp\left[j\frac{2\pi(z + 2f)}{\lambda} - j\frac{2\pi}{\lambda f}(x_s x + y_s y) - j\frac{\pi z}{\lambda f^2}(x_s^2 + y_s^2) \right], \qquad (1)$$

where λ is the light wavelength, f is the focal length of lens L1 and (x, y, z) are the coordinates behind the lens L1 with their origin at the rear focal point of the lens L1. The field $u(x,y,L)$ at the object mirror M1 and the field $u(x,y,L+2\Delta z)$ at the corresponding location in the other arm of the interferometer are imaged and superposed to form interference fringes on the CCD image sensor. Since each point source is completely incoherent to any other points on the source, the overall intensity on the image sensor contributed from all the source points is a sum of fringe intensities obtained from each point source:

$$\begin{aligned}
I(x, y, L) = \iint \bigg| &\frac{u_s(x_s, y_s)}{j\lambda f} \exp\left[j\frac{2\pi(L + 2f)}{\lambda} - j\frac{2\pi}{\lambda f}(x_s x + y_s y) - j\frac{\pi L}{\lambda f^2}(x_s^2 + y_s^2) \right] \\
&+ \frac{u_s(x_s, y_s)}{j\lambda f} \exp\bigg\{ j\frac{2\pi(L + 2\Delta z + 2f)}{\lambda} - j\frac{2\pi}{\lambda f}(x_s x + y_s y) \\
&\qquad - j\frac{\pi(L + 2\Delta z)}{\lambda f^2}(x_s^2 + y_s^2) \bigg\} \bigg|^2 dx_s dy_s, \qquad (2)
\end{aligned}$$

where the integration is performed over the area of the extend source. After a straightforward algebra the intensity

distribution given by Eq. (2) becomes

$$I\,(x,y,L) = B\left\{1 + |\mu(2\Delta z)|\cos\left[-\frac{4\pi\Delta z}{\lambda} + \phi(2\Delta z)\right]\right\}, \qquad (3)$$

where $B = \left(2/\lambda^2 f^2\right)\iint I_s(x_s, y_s)dx_s dy_s$. The function $\mu(\Delta z) = |\mu|\exp(j\phi)$ is the longitudinal complex degree of coherence given by

$$\mu(2\Delta z) = \frac{\iint I_s(x_s, y_s)\exp\left[j\frac{2\pi\Delta z}{\lambda f^2}(x_s^2 + y_s^2)\right]dx_s dy_s}{\iint I_s(x_s, y_s)dx_s dy_s}. \qquad (4)$$

From this analogy to the diffraction theory, our problem of producing high coherence for the optical path difference $2\Delta z$ can be reduced to the problem of finding a real and non-negative aperture distribution that produces a strong optical field on the optical axis at distance $2\Delta z$ from the rear focal point. Obviously a circular aperture whose transmittance has the form of the Fresnel zone plate can satisfy the above requirement if we chose

$$I_s(r_s) = \left(\frac{1}{2}\right)\left[1 + \cos\left(2\pi\gamma r_s^2 + \beta\right)\right] \qquad (5)$$

where $r_s^2 = x_s^2 + y_s^2$, and β is the initial phase of the zone plate. The zone plate illuminated by a plane wave focuses light on the axis at distances $\Delta z_o = 0,\ \pm 2\gamma\lambda f^2$ from the rear focal point. Correspondingly, a spatially incoherent source whose irradiance distribution has the same form as Eq.(5) produces the fields that exhibit high coherence for the three optical path differences $2\Delta z = \pm 2\lambda f^2\gamma$ and $\Delta z = 0$. By modulating the source distribution with a spatial light modulator and changing the zone plate parameter γ monotonically, we scan the coherence function along the Δz axis. When a high visibility peak is observed for some value γ_0 on the curve of visibility versus γ, it is a clear indication that the object mirror M1 is located at the distance $\Delta z = \lambda f^2\gamma_0$ from the reference mirror M2. Thus, by means of the spatial light modulator, we can control longitudinal spatial coherence without using mechanical moving components. If we assume a circular symmetric source and introduce a new radial parameter $\rho_s = r_s^2 = x_s^2 + y_s^2$, we have

$$\mu(\Delta z) \propto \left[\exp\left(\frac{j\pi R^2\Delta z}{\lambda f^2}\right)\sin c\left(\frac{\pi R^2\Delta z}{\lambda f^2}\right)\right] * \left[2\delta(\Delta z) + \exp(j\beta)\delta\left(\Delta z + \gamma\lambda f^2\right) + \exp(-j\beta)\delta\left(\Delta z - \gamma\lambda f^2\right)\right] \quad (6)$$

where sinc(x)=sin(x)/x, R is the radius of the circular source $I_s(\rho_s)$, $\delta(x)$ is the Dirac delta function, and * denotes convolution. Equation (6) gives three correlation peaks, and the distance between the central and side peaks can be

controlled by changing the parameter γ of the zone plate with a spatial light modulator.

2.2 New interpretation based on Haidinger fringes of equal inclination

In this section we give a new interpretation to the principle of the longitudinal coherence control, where the underlying physics for the coherence control is explained in terms of the Haidinger fringes of equal inclination. This new interpretation helps our intuitive understanding of the reason why the zone-plate-like spatially incoherent source generates the high coherence fields for the particular mirror distances Δz. In addition it provides an insight into the practical problem of how to design the specific shape of the zone plate when the optical system has aberrations and misalignments.
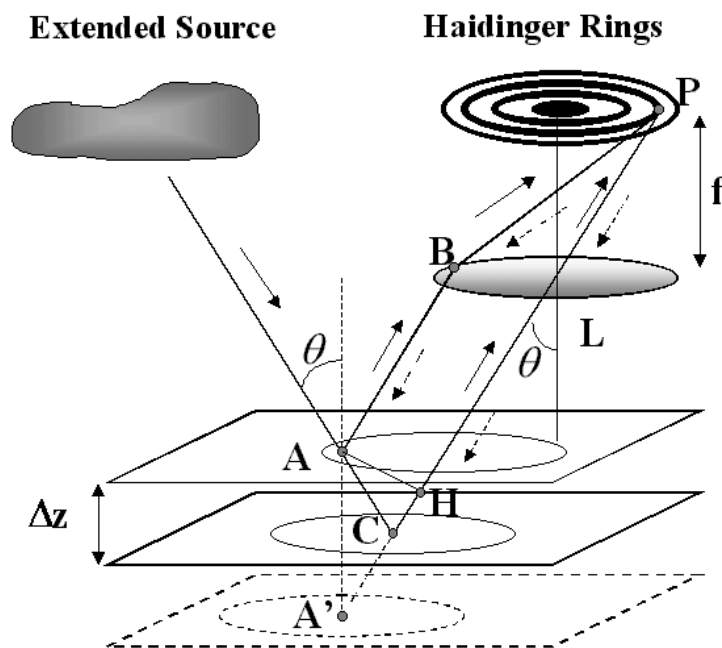

Fig.2. Generation of Haidinger fringes of equal inclination and its inverse process.

As shown in Fig.1, beam splitter BS forms a virtual image of the reference mirror M2 at distance Δz behind the object mirror M1, which serves as an effective reference mirror M2'. These two mirrors M1 and M2' together works as a plane parallel plate with optical thickness Δz. If the plane parallel plate is illuminated with an extended quasi-monochromatic spatially incoherent source, a set of Haidinger fringes of equal inclination (that is localized at infinity) will be observed in the focal plane of a lens L, as shown in Fig.2. A ray from the source that is incident on the plane parallel plate with a small angle θ is reflected by the upper and lower surfaces M1 and M2' to form parallel rays ABP and ACP. The optical path difference between these two rays is given by

$$\overline{ACH} = \overline{A'H} = 2\Delta z \cos\theta$$

$$\approx 2\Delta z\left(1 - \frac{\theta^2}{2}\right)$$

$$\approx 2\Delta z\left(1 - \frac{r^2}{2f^2}\right) \quad (7)$$

where r is the radial distance of the observation point P from the optical axis of the lens L, f is focal length of the lens, AH is a normal from point A to the ray CLP, and A' is a mirror image of point A with respect to the plane M2'. Thus the normalized intensity of the Haidinger fringes observed at point P is given by

$$I(r) = \left(\frac{1}{2}\right)\left[1 + \cos\left(\frac{2\pi\Delta z}{\lambda f^2}r^2 - \frac{4\pi\Delta z}{\lambda}\right)\right] \quad (8)$$

If we put $\gamma = \Delta z/\lambda f^2$ and $\beta = -4\pi\Delta z/\lambda$, we find that Eq.(8) has the same form as the Fresnel zone plate given by Eq.(5).

Let us now consider an inverse process in which the lens L is illuminated from backward by a point source at P on the observation plane. Being reflected by the lower surface, the ray PCA meets with the ray PBA at point A and interferes with each other. When the point source P is on the bright fringes of the Haidinger rings, the interference at point A is constructive because the optical path difference $\overline{ACH}$ is an integer multiple of the wavelength λ. Similarly, the interference becomes destructive if the point source is on the dark fringes of the Haidinger rings. If the lens L is illuminated with an extended quasi-monochromatic spatially incoherent source whose irradiance distribution is proportional to the intensity of the Haidinger fringes [given by Eq.(8)], then only the point sources located on the bright fringes participate in the interference. This means that, for every point source, interference occurs constructively, and uniform bright fringes are produced over the upper plane M1. Because the source is spatially incoherent, the bright fringes produced by the individual point sources are superposed on intensity basis. This in-phase superposition of many fringe intensities creates a spatially uniform bright fringe that is strongly localized on the upper plane M1. Since Eq.(8) does not change if Δz is replaced by $-\Delta z$, the same phenomenon will be observed when the plane M1 is located at the distance $-\Delta z$ below the plane M2'. When $\Delta z = 0$, the ray PBA overlaps with the ray PHC, and constructive interference occurs irrespective of the position of the point source P because the optical path difference is zero.

So far, for ease of understanding, we explained with the help of the virtual optical system shown in Fig.2 that includes virtual rays and a virtual mirror image of M2 formed by beam splitter BS. Based on this virtual optical system, we described as if real fringes were generated on the upper mirror plane M1. In the actual optical system shown in Fig.1, however, the fringes observed on the mirror plane M1 through the beam splitter from the side of CCD are virtual (rather

than real) fringes.   Therefore, we need a lens L2 that images the mirror plane M1 onto the CCD image sensor and converts the virtual fringes into the real fringes to be detected by the CCD sensor. Thus, referring to Fig.1, the extended incoherent source S, whose shape corresponds to the bright fringes of the Haidinger rings, produces an optical field that has a longitudinal coherence function with three peaks, which are observed when the distance between the two mirrors M1 and M2' is 0 or $\pm\Delta z$.

The interpretation given above permits one to determine the specific shape and the location of the source for an imperfect optical system that has aberrations and misalignments. When the optical system has aberrations, the source with the shape of a circular zone plate given by Eq.(5) is no longer the best choice because the Haidinger fringes do not have the perfect circular shape. Generally, we do not know what kind of aberrations is present and how they influence the optimum shape of the source. Even if the system is free from aberration, it is generally not easy to find the exact location of the optical axis of the system to which the center of the zone-plate-like source should be adjusted. Based on the new interpretation, we propose the following technique. Referring to Fig.1, we first illuminate the interferometer with another extended quasi-monochromatic source inversely from the side of the imaging lens L2 and the CCD camera, and record the Haidinger fringes generated on the plane S on which the designed source is to be placed. Then we use the recorded intensity distribution of the Haidinger fringes as the irradiance distribution $I_s(x_s, y_s)$ of the source to be placed on S. When we illuminate the interferometer with this source distribution $I_s(x_s, y_s)$ through the lens L1, we can generate an optical field that gives a high coherence peak for the mirror distance Δz for which the Haidinger fringes were recorded. If we record a set of the Haidinger fringes and generate the corresponding source distributions with a spatial light modulator, we can perform tomographic imaging at the desired mirror distances determined by the longitudinal spatial coherence function synthesized by the spatial light modulator.

3. EXPERIMENTS

Experiments have been conducted to demonstrate the validity of the principle. A schematic illustration of the experimental system is shown in Fig.3. A Michelson interferometer is illuminated by two quasi-monochromatic spatially incoherent light source, where one provides an extended source created by the beam from Laser 2, to generate the Haidinger fringes on the ground glass GG1; the other serves as a source for the spatial coherence synthesis. The two light sources are both He-Ne lasers with wavelength λ=0.6328μm. The beam from Laser1 was collimated by collimator C1 to illuminate a liquid crystal spatial light modulator (SLM) on which the Haidinger-fringe-like source irradiance distribution is displayed by a personal computer PC. The source irradiance distribution displayed on SLM is imaged by lens L1 onto the rotating ground glass plate GG1 to make a spatially incoherent source with the desired irradiance distribution. The light from each point on the ground glass is collimated by a lens L2, and is introduced into a Michelson interferometer. One mirror M1 was attached on a fixed arm to serve as an object mirror, and the other mirror M2 serves as a reference mirror. The mirror M2 was mounted on a piezo-electric transducer for phase shift, and the piezo-electric transducer itself was placed on a precision mechanical stage to form a variable arm. The two reflected

Laser 1   C1   L1   GG1   L2   M1   M2
P   SLM   BS1   PT
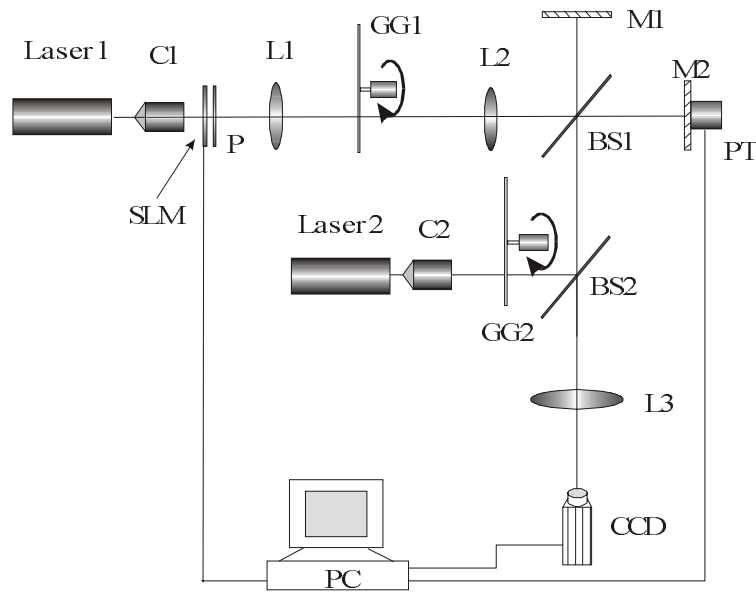Laser 2   C2   GG2   BS2
L3
CCD
PC

Fig.3. Schematic illustration of the experimental system:
C1,C2, collimator lens; SLM, spatial light modulator; GG1, GG2, ground glasses; PT, piezo-electric transducer.

beams from M1 and M2 were combined by the beam splitter BS1 and passed by the lens L3. The lens L3 forms an image of mirror M1 onto the CCD plane, so that intensity of the fringes virtually localized on the mirror M1 is recorded. According the principle described, the zone-plate-like distribution were generated by the personal computer and displayed on the spatial light modulator. The focal length of lens L2 was f=300mm. The experiments were performed as follows. At first we turned on Laser 2 only, and observed the Haidinger fringes on the ground glass GG1 by adjusting mirrors M1 and M2 exactly parallel. Subsequently, we produced a zone-plate-like pattern by computer according to the Haidinger fringes appearing on GG1, and displayed the zone-plate-like pattern on SLM. By this way, we made the designed zone plate and Haidinger fringes to match as closely as possible. Then turning off Laser 2 and switching on Laser 1, we observed fringes virtually localized on mirror M1 through the CCD camera with lens L3 focused on M1. The fringes have uniform illumination over the field of view because M1 and M2 have been made parallel, and they are high contrast because the source shape is tuned to the Haidinger fringes generated at the present mirror position. By moving the position of mirror M2, we changed the optical path difference between the two arms of Michelson interferometer and measured the visibility of the fringes by the phase-shift technique [12]. In this way, we obtained the distribution of degree of coherence along the axis.

Figure 4 (a) shows an example of the Haidinger fringes recorded by a CCD camera placed at the position of ground glass GG1. Due to the astigmatism introduced by the optical system, the Haidinger fringes have the shape of an ellipse, which can be modeled by the following equation:
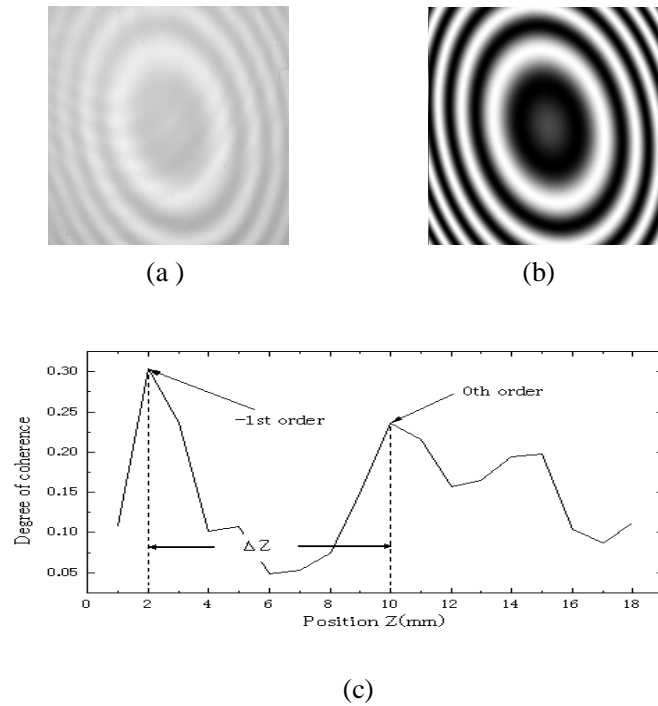
(a)   (b)

(c)

Fig.4. (a) Haidinger fringes recorded for $\Delta z = 8$ mm. (b) Source irradiance distribution designed to have the same shape with the Haidinger fringes. (c) Longitudinal degree of coherence. Optical path difference is zero, $\Delta z = 0$, at poisition z = 10mm on the horizontal axis.

$$I\left(x_s, y_s\right) \propto 1 + \cos\left\{2\pi\left[\gamma\left(x_s^2 + y_s^2\right) + A_0\left(x_s^2 - y_s^2\right) + B_0 x_s y_s\right] + \beta\right\} \qquad (9)$$

where A_0 and B_0 parameterize the astigmatism, and the parameters γ and β correspond to those of an ideal zone plate in Eq.(5). If we remember Eq.(5) that gives $\gamma = \Delta z / \lambda f^2$ in the aberration-free case, we can expect from Eq.(9) that, as we reduce the mirror distance, the elliptic fringe pattern will change its shape and becomes hyperbola for $\Delta z = 0$. If we move the mirror further beyond to the region of $-\Delta z$, the fringe pattern will become ellipses again but with their major and minor axes being exchanged. This is indeed what we observed by experiment. From this phenomenon we identified the location of $\Delta z = 0$ to be at 10mm of the dial reading of the stage. Note that, just as the temporally incoherent white-light source does, a quasi-monochromatic spatially incoherent source provides information about the location of $\Delta z = 0$. The Haidinger fringes shown in Fig.4(a) is recorded for $\Delta z = 8$ mm (which corresponds to the stage dial reading of 2mm). Figure 4.(b) shows the irradiance distribution of the source designed by computer, which has the same shape as the Haidinger fringes in Fig.4(a). Moving the stage by 1mm steps, we measured the

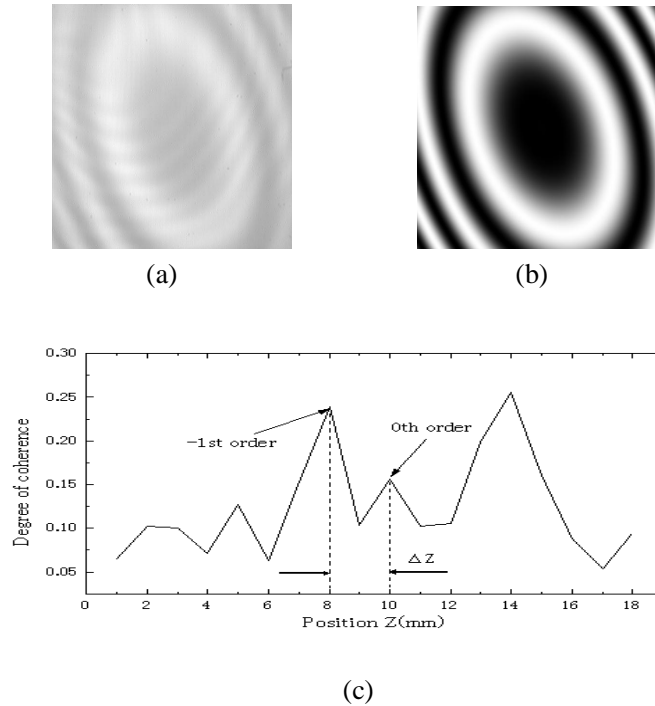(a)   (b)

(c)

Fig.5 (a) Haidinger fringes recorded for $\Delta z = 2$ mm. (b) Source irradiance distribution designed to have the same shape with the Haidinger fringes. (c) Longitudinal degree of coherence. Optical path difference is zero, $\Delta z = 0$, at poisition z = 10mm on the horizontal axis.

coherence function (the fringe contrast) by using the phase-shift technique [12]. The result is shown in Fig.4(c). As designed, a coherence peak is observed at the position of 2mm in the stage dial reading that corresponds to $\Delta z = 8$ mm. The peak for $\Delta z = 0$ is also observed at the correct position 10mm in the stage dial reading, but the peak height is lower than that for $\Delta z = 8$ mm. The peak for $\Delta z = -8$ mm is not clearly observed. This can be explained by the degree of overlap of the source shape (or the shape of the Haidinger fringes) for $\Delta z = 8$ mm with those for $\Delta z = 0$ and $\Delta z = -8$ mm. We can observe the lower peak for $\Delta z = 0$ because the ellipse for $\Delta z = 8$ mm has some overlapping area with the hyperbola for $\Delta z = 0$. On the other hand, the ellipse for $\Delta z = 8$ mm has much less overlapping area with the ellipse for $\Delta z = -8$ mm because their major and minor axes are exchanged. Similarly, the Haidinger fringes for $\Delta z = 2$ mm and the corresponding source irradiance distribution are shown in Fig.5 (a) and (b), respectively. Here again we observe a coherence peak at the position 8mm that corresponds to $\Delta z = 2$ mm. The relation between the parameter γ and the mirror distance Δz for the coherence peak was plotted as shown in Fig.6. With the change of the parameter γ, other parameters A_0 and B_0 were changed by the same factor. Because of astigmatism, Δz is not exactly proportional to the parameter γ, but Δz increases linearly with γ. This means that even for an optical system with astigmatism, the position of the coherence peak can be controlled by the spatial frequency of the zone plate.
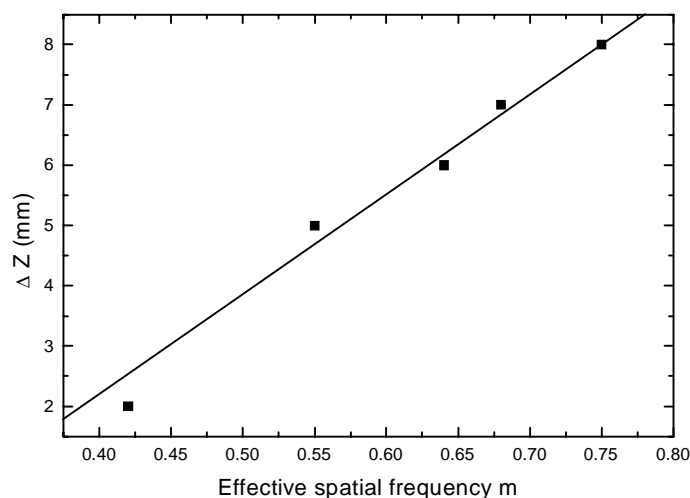
Fig.6   The relationship between the optical path difference for the first coherence peak and effective spatial frequency.

4. CONCLUSION

We have proposed a new method for controlling longitudinal degree of coherence that has the potential application in tomography by changing source intensity distribution with spatial light modulator. Unlike conventional techniques used for the measurement of surface profiles, the proposed technique permits tomographic measurement without changing the optical path difference between the two arms of the interferometer. The proposed interferometric system has a unique characteristic that high contrast fringes are created only at locations where both the surface height and the local surface inclination satisfy the particular conditions set by the structure of the zone-plate-like source and the orientation of the reference mirror. This characteristic has potential application to the simultaneous detection of the distance and the local surface inclination of an object. We have presented a new interpretation to the principle, and proposed a solution to the source alignment issues based on the new interpretation.

ACKNOWLEDGMENTS

REFERENCES

1. R.C. Youngquist, S. Carr, and D. E. N. Davies, "Optical coherence-domain reflectometry: a new optical evaluation technique," Opt. Lett. **12**, 158-160 (1987).

2. D Huang, E. A. Swanson, C. P. Lin, J. S. Schuman, W. G. Stinson, W. Chang, M. R. Hee, T. Flotte, K. Gregory, C. A. Puliafito, and J. G. Fujimoto, "Optical coherence tomography," SCIENCE **254**, 1178-1181 (1991).

3. B. S. Lee and T. C. Strand, "Profilometry with a coherence scanning microscope," Appl. Opt. **29**, 3784-3788 (1990).

4. T. Dresel, G. Hausler, and H. Venzke, "Three-dimensional sensing of rough surfaces by coherence radar," Appl. Opt. **31**, 919-925 (1992).

5. L. Mandel and E. Wolf, *Optical coherence and quantum optics*, 1st ed. (Cambridge 1995) Chap. 4, p. 149.

6. M. Takeda, "The philosophy of fringes – analogies and dualities in optical metrology," Fringe `97, Proc. Third International Workshop on Automatic Processing of Fringe Patterns, W. Jueptner and W. Osten Ed., Akademie Verlag Berlin, 17-26 (1997).

7. C. W. McCutchen, "Generalized source and the Van Cittert-Zernike theorem: A study of the spatial coherence required for interferometry," J. Opt. Soc. Am. **56**, 727-733 (1966).

8. J. Rosen and A. Yariv "General theorem of spatial coherence: application to three-dimensional imaging" J. Opt. Soc. Am. A, **13**, 2091-2095 (1996).

9. J. Rosen and A.Yariv "Longitudinal partial coherence of optical radiation," Opt. Comm. **117**, 8-12 (1995).

10. J. Rosen and M. Takeda "Longitudinal spatial coherence applied for surface profilometry," Appl. Opt. **39**, 4107-4111 (2000).

11. K. Hotate and T. Okugawa, "Optical information-processing by synthesis of the coherence function," J. Lightwave Tech. **12,** 1247-1255 (1994).

12. J. H. Bruning, D. J. Herriott, J. E. Gallagher, D. P. Rosenfeld, A. D. White, and D. J. Brangaccio "Digital wavefront measurement interferometer," Appl. Opt. **13**, 2693-2703 (1974).